

THE HYPERFINE STRUCTURES OF RUBIDIUM ATOM USING ELECTROMAGNETICALLY INDUCED TRANSPARENCY

NGUYEN THI DIEU HIEN*

ABSTRACT

In this paper, we studied the hyperfine structures of the Rubidium in D states $5D_{5/2}$, $7D_{3/2}$, $7D_{5/2}$ using Electromagnetically Induced Transparency (EIT). In order to improve the EIT signal-to-noise ratio, the laser frequency was stabilized to a Rubidium hyperfine transition while the coupling laser scanned the transition of excited states. We compared the experimental data with the simulation one.

Keywords: Hyperfine Structures, Rubidium, Electromagnetically Induced Transparency.

TÓM TẮT

Cấu trúc siêu tinh tế của phân tử Rubidium sử dụng tính trong suốt cảm ứng điện từ

Trong bài báo này, chúng tôi nghiên cứu về cấu trúc siêu tinh tế của Rubidium ở trạng thái D $5D_{5/2}$, $7D_{3/2}$, $7D_{5/2}$ bằng tính trong suốt cảm ứng điện từ. Trong thí nghiệm này, để cải thiện EIT so với nhiễu loạn, tần số của laser sẽ được ổn định ở một chuyển tiếp siêu tinh tế trong khi laser coupling sẽ quét qua các chuyển tiếp của trạng thái kích thích. Chúng tôi so sánh các kết quả thí nghiệm với mô phỏng.

Từ khóa: Cấu trúc siêu tinh tế, Rubidium, tính trong suốt cảm ứng điện từ.

1. Introduction

The hyperfine structure is a phenomenon resulting to the splitting in energy levels of atoms, molecules and ions. In an atom, the hyperfine structure is caused by the nuclear magnetic dipole moment in a magnetic field. Each of these energy levels may be assigned a quantum number, and they are then called quantized levels. The hyperfine structure of an atom is usually defined over eigenstates $\{f, J, I, F, m_F, g\}$. The hyperfine structures of Rubidium-87 are studied in many techniques such as quantum beats [8], based on the hyperfine interaction without any external magnetic fields, the two-photon transitions [4], etc. In this work, we would like to use the phenomenon of EIT in ladder type to study the hyperfine spectroscopy of upper states in Rubidium atom. In this technique, the probe laser couples the ground state to an intermediate state and the coupling laser couples two excited states.

The phenomenon of EIT was first observed by Boller, Imamoglu, and Harris in 1991 in strontium vapor [1]. EIT has presented in recent years by its applications in atomic physics and quantum optics such as optical switches [7], lasing without

*M.Sc., HCM City International University; Email: ntdhien@hcmiu.edu.vn

population inversion [5], and quantum information [6]. In this paper, we studied the hyperfine structures in D-states of Rubidium atoms $5S_{1/2} \rightarrow 5P_{3/2} \rightarrow 5D_{5/2}$, $5S_{1/2} \rightarrow 5P_{3/2} \rightarrow 7D_{3/2}$ and $5S_{1/2} \rightarrow 5P_{3/2} \rightarrow 7D_{5/2}$ at room temperature. We used the Mathematica program to simulate the EIT by solving Bloch equation and considering the integration over Doppler velocity distribution.

2. Theory

EIT originates from the Induced Transparency in an absorbing medium by a weak probe field, coupled by a strong coupling field. The transitions between the levels $|1\rangle$, $|2\rangle$, and $|3\rangle$ are allowed electric dipole transitions, the $|1\rangle \rightarrow |3\rangle$ transition is always a dipole forbidden transition because $|3\rangle$ is a metastable state. To study EIT, we used the density matrix approach with derived Rabi oscillation and the probability amplitude in the system would transfer between states, interfere destructively [3]. Another approach is the dressed state picture, which is the interaction between atoms and photons [2]. The ladder type has been studied actively in this time and the Doppler-free configuration in a ladder-type system can be obtained when the probe and coupling fields are counter-propagating. The ladder type is mainly applied to study the hyperfine structure of the excited state. Generally, the energy difference among hyperfine states in an excited state is smaller than the ground state. We studied the three level systems with Ω_c , Ω_p , ω_c , ω_p being Rabi frequencies, frequencies of coupling and probe laser. The decay rates of the intermediate and excited state are Γ_2 and Γ_3 , and $\Gamma_3 = \Gamma_{31} + \Gamma_{32}$. Δ_c and Δ_p are the frequency detunings of coupling and probe laser, and $\Delta_c = \omega_{32} - \omega_c$ and $\Delta_p = \omega_{21} - \omega_p$. Therefore, by using the Mathematica program, we could solve the Bloch equation.

In room temperature vapor cell, we need to consider the thermal velocity distribution [9]. Atom is moving with velocity v in the same direction with the probe beam. The probe and coupling beams are counter-propagating. According to the Doppler shift, the probe and coupling detunings become

$$\begin{aligned}\Delta_p &\rightarrow \Delta_p - v/\lambda_p, \\ \Delta_c &\rightarrow \Delta_c + v/\lambda_c.\end{aligned}$$

Therefore,

$$\rho_{21} = \frac{\Omega_p/2}{(\Delta_p - v/\lambda_p) - i\frac{\Gamma_{21}}{2} - \frac{(\Omega_c/2)^2}{(\Delta_p + \Delta_c) + v(1/\lambda_p - 1/\lambda_c) - i(\Gamma_{31} + \Gamma_{32})/2}} \quad (1)$$

Obviously, ρ_{21} is proportional to the weak probe field and known as the strength from state 1 to state 2. The linewidth will get smaller by counting the thermal velocity distribution.

$\rho_{21}(int) = \frac{1}{\sqrt{\pi}u} \int_{-\infty}^{\infty} Im[\rho_{21}] e^{-\left(\frac{v}{u}\right)^2} dv$ (2), where $u = \sqrt{2k_B/m}$ is the most probable velocity, k_B is Boltzmann constant, and m is the atomic mass.

3. Experimental setup

The experimental setup was shown in Figure 1. The ladder type of ^{87}Rb atoms was studied at room temperature with a length cell of 10 cm. The probe field was provided by an external cavity diode laser (Toptica DL 100) with 0.5 MHz linewidth at 780.2 nm. The coupling field was given by a continuous wave (cw) Ti: Sapphire ring laser (776.0 nm), pumped by Verdi-10 or a tunable cw Dye Ring laser (R6G dye) (Coherent. 899-21) at 572.62 nm or 572.57 nm. The frequency of the probe beam was stabilized by a Doppler-free saturation absorption technique and locked at $|5S_{1/2}, F = 2\rangle \rightarrow |5P_{3/2}, F' = 3\rangle$.

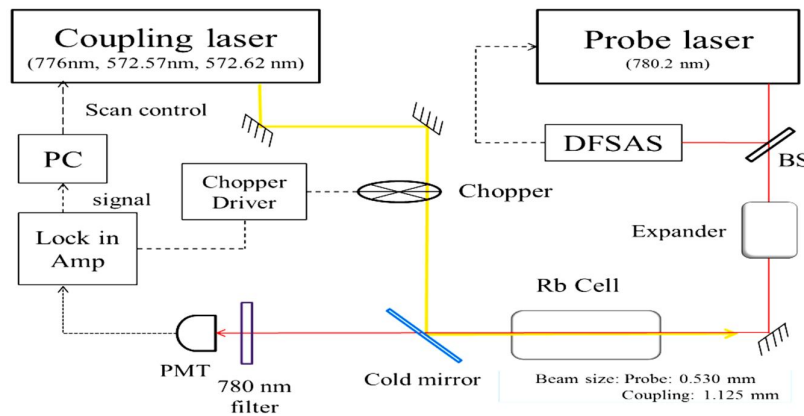


Figure 1. Experiment Setup for EIT Rubidium. BS: beam splitter; PMT: photomultiplier tubes

The probe and coupling beams were counter propagating through the Rb vapor cell. The expander was used in the probe laser to reduce the beam size of the probe. The beam size of the probe laser was 0.530 mm and the coupling beam was 1.125 mm. In this experiment, the cold mirror which allowed the visible light to be reflected and infrared light transmitted, made the coupling beam and the probe beam totally overlap. The coupling field was modulated by a chopper at 1.00 kHz and demodulated by the lock-in amplifier (Stanford Research System, SR 830). Therefore, the EIT signal improved signal-to-noise ratio and be recorded at a personal computer (PC) using the LabVIEW program. The photomultiplier tube (PMT) was used to detect the EIT signal by taking the weak probe field with the transmission of the coupling field. A band pass filter was used in front of the PMT to block the other light surrounding with the range of 780 ± 5 nm.

4. Results and Discussions

The experimental result of EIT in transition $5S_{1/2} \rightarrow 5P_{3/2} \rightarrow 5D_{5/2}$ with coupling scanning frequency range of 100 MHz is shown in Figure 2.

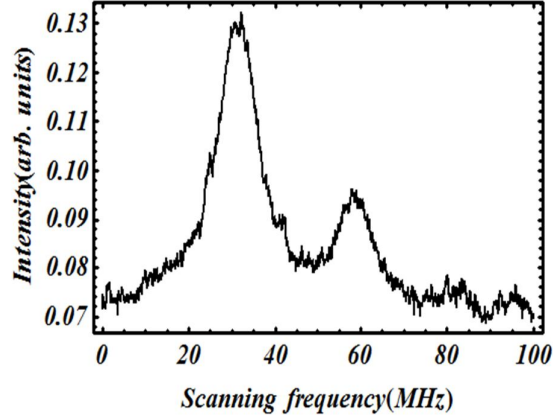


Figure 2. EIT of $5S_{1/2} \rightarrow 5P_{3/2} \rightarrow 5D_{5/2}$

The probe beam is locked at $|5P_{1/2}, F = 2\rangle$ to $|5P_{3/2}, F' = 3\rangle$, Δ_p will be blue detuning with the group velocity caused by Doppler Effect. Electromagnetically Induced Transparency occurs when the coupling laser has the same velocity with the atom velocity. The probe detuning is $\Delta_p = -\omega_p(v_z/c)$, where ω_p is the frequency of probe laser, v_z is the velocity of the atom in z direction, c is the speed of light. The coupling detuning can be calculated by $\Delta_c = -(\lambda_p/\lambda_c)\Delta_p$, where λ_p and λ_c are the wavelengths of probe and coupling beams, λ_p/λ_c is the wavelength mismatching factor. Therefore, we can predict all the peak positions based on the non-stationary atom with the error smaller than 3%.

We can identify all the peak positions based on the non-stationary atom. We assume the transition $|5S_{1/2}, F = 2\rangle \rightarrow |5P_{3/2}, F' = 3\rangle \rightarrow |5D_{5/2}, F'' = 3\rangle$ which is labeled as $23'4''$ is on resonance. All the peak positions $22'3''$, $23'3''$, $21'2''$, $22'2''$, $23'2''$, $21'1''$, $22'1''$ will be calculated by the order showed in Figure 3.

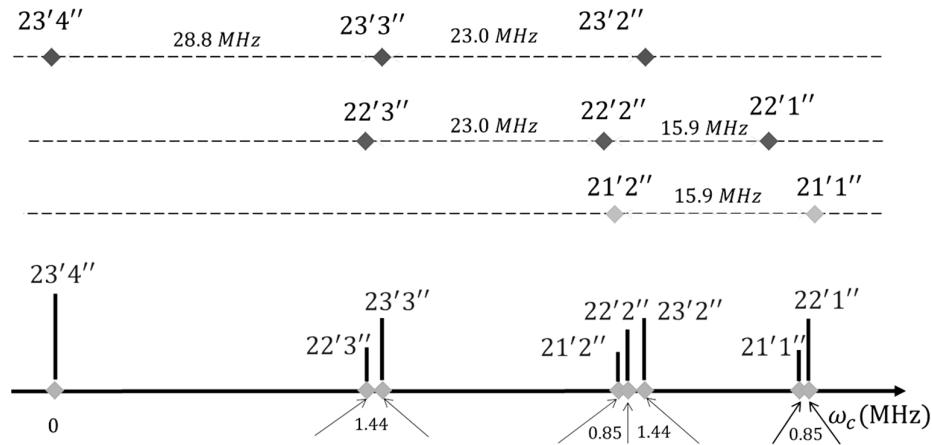


Figure 3. All peak positions of $5S_{1/2} \rightarrow 5P_{3/2} \rightarrow 5D_{5/2}$

In the simulation, we studied the EIT signal by taking the exponential part with the integration of the imaginary part of ρ_{21} , $\int_{-\infty}^{\infty} \text{Im}[\rho_{21}] e^{\left(\frac{\nu}{u}\right)^2} d\nu$ caused by the non stationary Rubidium atom in the cell. We used these simulation parameters: $\Gamma_2 \rightarrow 6.06$ MHz, $\Gamma_3 \rightarrow 0.97$ MHz. The simulation included the probability amplitude so that each transition will come out with different intensity amplitude. Figure 4 is the combination between experimental and simulation results. The final state $|5D_{5/2}, F'' = 4\rangle$ has the highest intensity while the state $|5D_{5/2}, F'' = 1\rangle$ has less intensity. This result is caused by the transition probability. In three sets of final states $F'' = 4, F'' = 2, F'' = 1$, EIT is created the same linewidth and intensity. In peak $F'' = 3$, the intensity of experiment is higher than the simulation. In general, the theory concept agreed with the experiment results and gives a good explanation about labeling the peak positions.

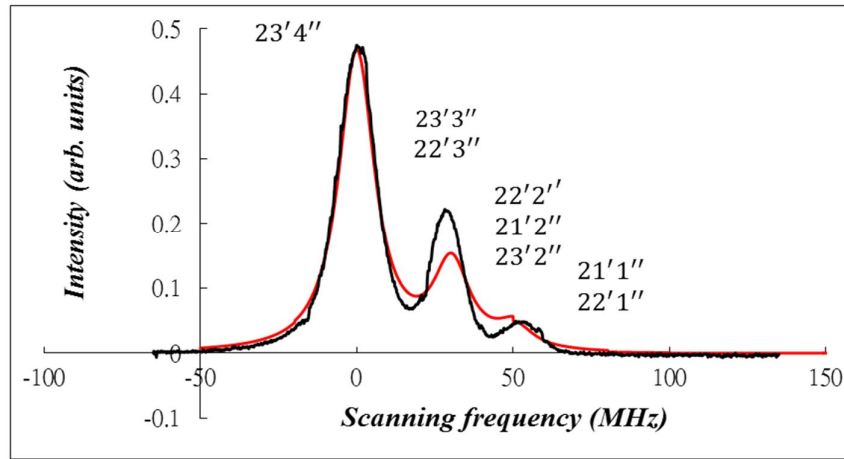


Figure 4. The EIT at transition $5S_{1/2} \rightarrow 5P_{3/2} \rightarrow 5D_{5/2}$, the black line is the experimental data and the red line represents the simulation result

In case the coupling beam power is 52 mW and the probe is 1.25 μW , the EIT of $5S_{1/2} \rightarrow 5P_{3/2} \rightarrow 7D_{3/2}$ is observed in Figure 5. EIT peaks are influenced by the two-photon probability, so we can just get one peak in the $F'' = 3$. We compared the result between the theory and the experiment with $\Gamma_2 = 6.06$ MHz, $\Gamma_3 = 0.46$ MHz, $\Omega_p = 0.15$ MHz, $\Omega_c = 44.0$ MHz, dephasing rate $\gamma = 18$ MHz, which changes the linewidth of the EIT spectrum, has the value 20 MHz. In Figure 5, the EIT spectrum in the simulation and the experiment can fit in the linewidth 56 MHz but the dips in two wings could not fit very well.

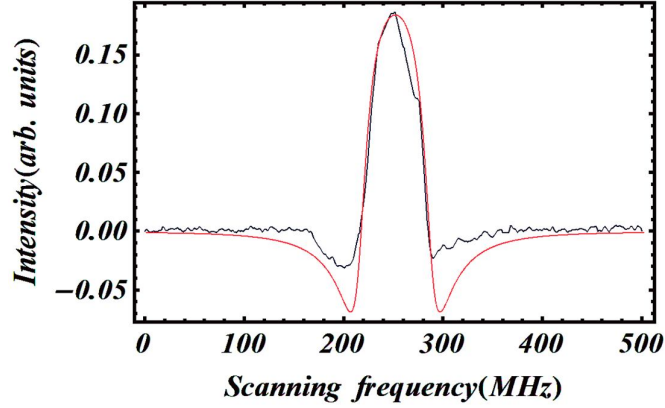


Figure 5. The EIT of $5S_{1/2} \rightarrow 5P_{3/2} \rightarrow 7D_{3/2}$, the black line is the experimental data and the red line represents the simulation result

The result of EIT ladder type for the transition $5S_{1/2} \rightarrow 5P_{3/2} \rightarrow 7D_{5/2}$ is given by the scanning coupling beam at a power of 68 mW and the probe power of 39.9 nW with the scanning range of 500 MHz. The wavelength mismatching factor is $\lambda_p/\lambda_c = 1.3$ and $|5S_{1/2}, F = 2\rangle \rightarrow |5P_{3/2}, F' = 3\rangle \rightarrow |5D_{5/2}, F'' = 3(4)\rangle$ is on resonance EIT signal.

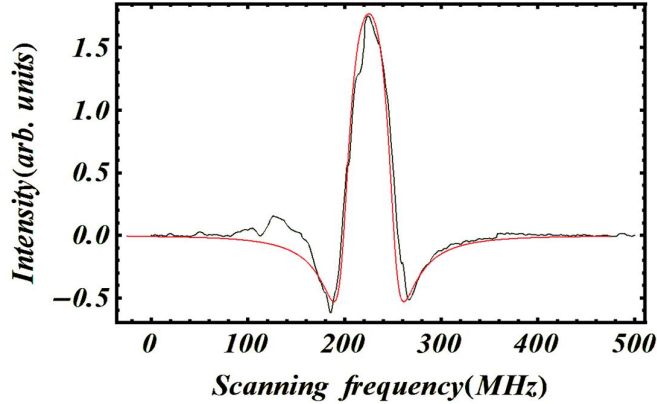


Figure 6. The EIT of $5S_{1/2} \rightarrow 5P_{3/2} \rightarrow 7D_{5/2}$, the black line is the experimental data and the red line represents the simulation result

From Figure 6, we will compare the experimental and simulation results by adding three peaks $23'4''$, $23'3''$ and $23'2''$ into one peak. Both experiment and theory can fit well the linewidth of 62 MHz.

The EIT spectrum in this work mainly identifies the hyperfine structure for the excited state in ^{87}Rb . In the $5S_{1/2} \rightarrow 5P_{3/2} \rightarrow 5D_{5/2}$ transition, we can clearly label the peak positions of each transition by adding the non-stationary atom. The wavelength mismatching factor (Δ_p/Δ_c) caused the dips of EIT signals. In our experiment, the strong dips can get with $\Delta_p/\Delta_c = 1.362$ in $5S_{1/2} \rightarrow 5P_{3/2} \rightarrow 7D_{3/2}$ and $5S_{1/2} \rightarrow 5P_{3/2} \rightarrow 7D_{5/2}$ and no dips in the case wavelength mismatching factor $\Delta_p/\Delta_c = 1.005$ with transition

$5S_{1/2} \rightarrow 5P_{3/2} \rightarrow 5D_{5/2}$. In the transitions $5S_{1/2} \rightarrow 5P_{3/2} \rightarrow 7D_{3/2}$ and $5S_{1/2} \rightarrow 5P_{3/2} \rightarrow 7D_{5/2}$, we would like to study further by adding the temperature factor. The Mathematica program is used to simulate our experiment and it can fit very well with the experimental data. In the transition $5S_{1/2} \rightarrow 5P_{3/2} \rightarrow 5D_{5/2}$, the width of EIT and the intensity fit very well in the case of $F'' = 4$, $F'' = 2$ and $F'' = 1$. However, in case of $F'' = 3$, the intensity simulation is smaller than the experimental result. In the transition $5S_{1/2} \rightarrow 5P_{3/2} \rightarrow 7D_{3/2}$, the linewidth can fit in the experiment and the simulation but the dips of the experiment looks smaller comparing with the simulation. In case of transition $5S_{1/2} \rightarrow 5P_{3/2} \rightarrow 7D_{5/2}$, both the linewidth and the dips in the experiment and the simulation are the same.

4. Conclusion

In this paper, the EITs of Rubidium in D states $5S_{1/2} \rightarrow 5P_{3/2} \rightarrow 5D_{5/2}$, $5S_{1/2} \rightarrow 5P_{3/2} \rightarrow 7D_{3/2}$ and $5S_{1/2} \rightarrow 5P_{3/2} \rightarrow 7D_{5/2}$ were observed at room temperature. Our results made the comparison between the experiment and the simulation, which gave a better understanding of the hyperfine structures of Rubidium atom. The difference in intensity of EITs can be explained by adding the theory of optical pumping. We will study more in detail about the theory of optical pumping.

REFERENCES

1. A. Imamoglu and S. E. Harris (1989), "Observation of Electromagnetically Induced Transparency", *Opt. Lett.* 14, 1344.
2. C. Cohen-Tannoudji, J. Dupont-Roc, and G. Grynberg (1992), *Atom-Photon Interactions: Basic Process and Applications*, Wiley Press, New York.
3. J.J. Sakurai (1994), *Advanced quantum mechanics*, Addison and Wesley.
4. M. J. Snadden, A. Bell, E. Riis, and A. Ferguson (1996), "Two-photon spectroscopy of laser-cooled Rb using a mode-locked laser", *Opt. Commun.* 125, 70.
5. O. Kocharovskaya (1992), "Amplification and lasing without inversion", *Phys. Rev.* 219, 175.
6. R. G. Beausoleil, W. J. Munro, D. A. Rodrigues, and T. P. Spiller (2004), "Applications of Electromagnetically Induced Transparency to quantum information processing", *J. Mod. Opt.*, 51, 2441.
7. S. E. Harris and Y. Yamamoto (1998), "Photon switching by quantum interference", *Phys. Rev. Lett.*, 81, 3611.
8. W. A. van Wijngaarden, J. Li, and J. Koh (1993), "Hyperfine-interaction constants of the $8D_{3/2}$ state in ^{85}Rb using quantum-beat spectroscopy", *Phys. Rev.*, A 48, 829.
9. Z. S. He, J. H. Tsai, Y. Y. Chang, C. C. Liao, and C. C. Tsai (2013), "Ladder-type Electromagnetically Induced Transparency with Optical Pumping Effect", *Phys. Rev.* A 87, 033402.

(Received: 21/9/2015; Revised: 12/10/2015; Accepted: 22/12/2015)